PAPER • OPEN ACCESS

Ultrafast transient dynamics in composite multiferroics

View the article online for updates and enhancements.

You may also like

New Journal of Physics

The open access journal at the forefront of physics

CrossMark

PAPER

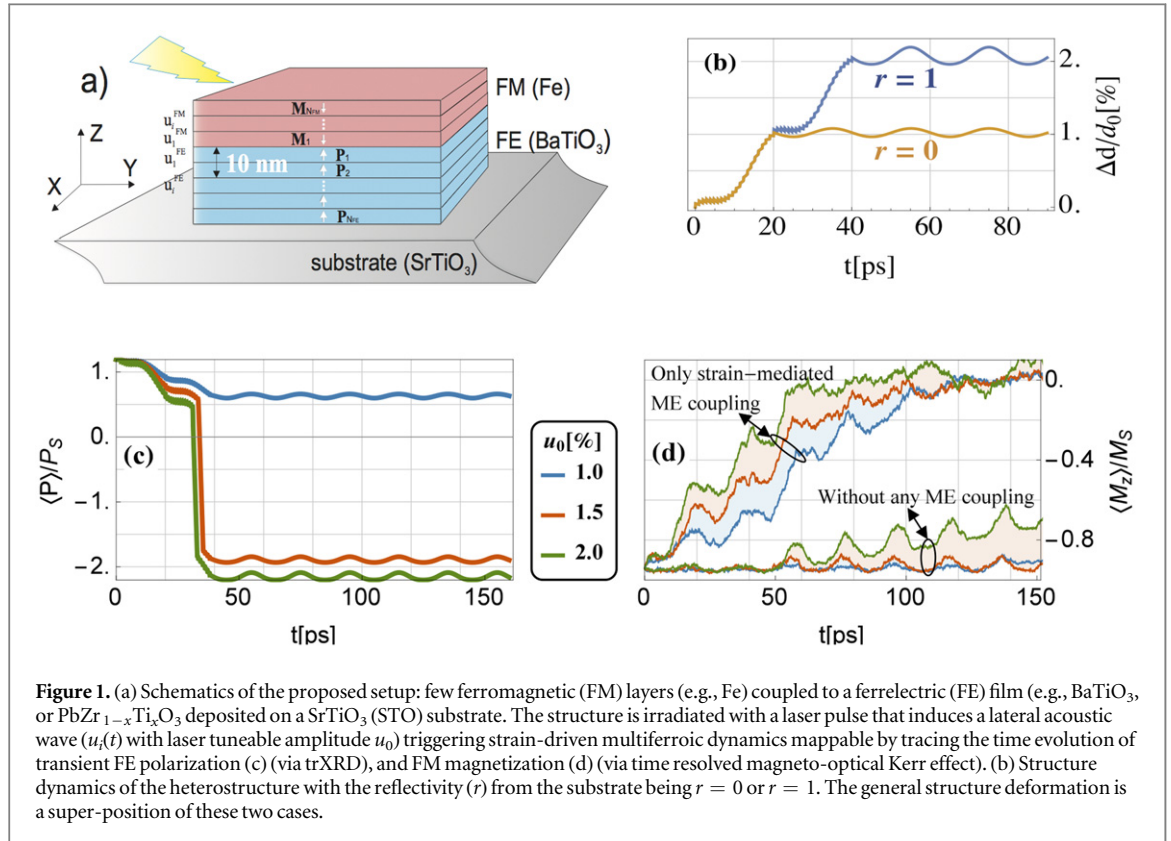# Ultrafast transient dynamics in composite multiferroics

Chenglong Jia[1,2,3], Ning Zhang[1], Alexander Sukhov[2] and Jamal Berakdar[2]

1   Key Laboratory for Magnetism and Magnetic Materials of MOE, Lanzhou University, Lanzhou 730000, People's Republic of China
2   Institut für Physik, Martin-Luther Universität Halle-Wittenberg, D-06099 Halle, Germany
3   Author to whom any correspondence should be addressed.

E-mail: cljia@lzu.edu.cn

Keywords: muliferroics, piezoelectricity, strain pulses, magnetostriction

Abstract

We investigate theoretically the dynamic multiferroic (MF) response of coupled ferroelectric (FE)/ferromagnetic (FM) composites upon excitation by a photo-induced acoustic strain pulse. Two magnetoelectric (ME) mechanisms are considered: interface strain- and charge-mediated ME couplings. The former results in demagnetization, depolarization and repolarization within tens of picoseconds via respectively magnetostriction and piezoelectricity. Charge ME interaction affects the FE/FM feedback response leading to magnetization recovery. Experimental realization based on time-resolved x-ray diffraction is suggested. The findings indicate the potential of composite MF for photo-steered, high-speed, multi-state electronic devices.

Introduction

Appropriately synthesized ferroelectric (FE) and ferromagnetic (FM) multilayer or nano structures may show a multiferroic (MF) (magnetic, electric, and/or elastic) response which is indicative of an emergent coupling between the respective order parameters [1–12]. In addition to the fundamental questions regarding the origin of the underlying physics, this observation holds the promise of qualitatively new device concepts. MF memory devices [13] with multi-state data storage and heterogeneous read/write capability through the interfacial strain effects [14–18], the direct electric field effects [19–27], and exchange-bias [28–30] are a few examples. A key element thereby is the strength and symmetry of MF coupling and whether it is utilizable for swiftly transferring/converting FM into FE information. Time-resolution, particularly how fast such a conversion may take place and how to map it in practice are issues that have not been addressed yet theoretically for MF composites, despite the intense research on MF materials. This work contributes to this aspect by making a specific proposal for an experiment and provides theory and numerical simulations to unveil the time scale of mediating information (excitation) via MF coupling. Recently, first time-resolved x-ray diffraction (trXRD) experiments were conducted to access the time-resolved FE response and lattice dynamics in single phase MF $BiFeO_3$ film [31, 32]. Photo-induced stabilization and enhancement of FE polarization were observed for $Ba_{0.1}Sr_{0.9}TiO_3/La_{0.7}Ca(Sr)_{0.3}MnO_3$ [33]. Our focus here is on layered FE/FM composites (see figure 1) whose magnetoelectric (ME) interaction may stem from the interfacial strain effects and/or spin rearrangement [4, 6, 9, 27].

For isolated FM systems, the ultrafast laser-induced magnetization dynamics (i.e. roughly speaking, a femtosecond demagnetization, a picosecond recovery, and a picosecond to nanosecond magnetization precession and relaxation) are intensively studied with important implications for photo-magnetic devices [34]. For FE nanostructured materials, the ultrafast mechanical and electronic dynamics are well documented [35, 36]. An optical pump excitation pulse generates a propagating mechanical stress, which results in picosecond polarization dynamics [37–39] that can be probed experimentally via trXRD. In composite MFs, it is yet to be clarified how upon such a pump pulse the coupled time-resolved MF dynamics are manifested, an issue addressed here.

Figure 1. (a) Schematics of the proposed setup: few ferromagnetic (FM) layers (e.g., Fe) coupled to a ferrelectric (FE) film (e.g., BaTiO$_3$, or PbZr$_{1-x}$Ti$_x$O$_3$ deposited on a SrTiO$_3$ (STO) substrate. The structure is irradiated with a laser pulse that induces a lateral acoustic wave ($u_i(t)$ with laser tuneable amplitude u_0) triggering strain-driven multiferroic dynamics mappable by tracing the time evolution of transient FE polarization (c) (via trXRD), and FM magnetization (d) (via time resolved magneto-optical Kerr effect). (b) Structure dynamics of the heterostructure with the reflectivity (r) from the substrate being $r = 0$ or $r = 1$. The general structure deformation is a super-position of these two cases.

Generalities and proposed setup

Experimentally, FE/FM MF heterostructures were successfully realized and characterized [1–4, 9–11]. In principle, strain and charge co-mediated ME coupling are expected in composite MFs [40]. The direct charge-mediated ME interaction is generally due to the induced changes in the magnetic states by the electrostatic screening effect [9, 27] it is however strong and plays a dominant role in some FE/FM-metal systems [42–45]. Whereas, the piezoelectric strain is found to give rise to an electrically tunable uniaxial magnetic anisotropy [9, 18, 40]. To unveil the transient dynamics we propose in figure 1 to employ photo-induced transient strain and trXRD and monitor the effects of interface strain- and charge-mediated ME couplings. The strain can be chosen lateral, as in our case, or as having in-plane components by an additional appropriate grating atop the FM film. For strain-induced magnetization dynamics in conventional isolated FM we refer to [46] and references therein. Calculations show, for a MF composite chain electrically induced magnetization reversal is not achievable for large/thick FM subsystem [18, 47]. This is because of the interface-limited nature of MF coupling [9, 27]. Therefore, it is advantageous to choose a system consisting of a thin FM layer (such as Fe with thickness $d_{FM} = 10$ nm) and a thicker FE layer (e.g. PbZr$_{1-x}$Ti$_x$O$_3$ (PZT) or BaTiO$_3$ (BTO) with thickness $d_{FE} = 100$ nm) grown epitaxially on a substrate SrTiO$_3$ (STO) (figure 1(a)). Fe[110] can be caped (with thin transplant Au-layer to prevent oxidation) and rotated to align parallel to BTO[100], resulting in in-plane misfit strains[4] $u_\parallel^{Fe} = 1.39\%$ and $u_\parallel^{BTO} = -0.139\%$. The normal strains are determined by the Poisson ratio, $n_{Fe} = u_\parallel^{Fe}/u_z^{Fe}$ and $n_{BTO} = u_\parallel^{BTO}/u_z^{BTO}$ with $n_{Fe} = 0.26$ [48] and $n_{BTO} = 0.65$ [49], respectively. In the following we focus on the particular situation where the spontaneous FE polarization is directed perpendicular to the substrate plane (hereafter referred to as the $\mathbf{e}_z$-direction).

From a computational point of view, the coarse-graining procedure with cell size $a = 5$ nm is conveniently used to obtain the macroscopic quantities of polarization $\mathbf{P}_i$ (with $i = 1,...,N_{FE}$ and $N_{FE} = d_{FE}/a$) and magnetization $\mathbf{M}_j$ (with $j = 1,...,N_{FM}$ and $N_{FM} = d_{FM}/a$) [50]. The change in polarization $\mathbf{P}_i$ to a first-order approximation can then be understood in terms of piezoelectricity [51]

---

[4] The in-plane misfit strains are estimated by, $u_\parallel^{Fe} = -(a_\parallel - a_0^{Fe})/a_\parallel = 1.39\%$ and $u_\parallel^{BTO} = -(a_\parallel - a_0^{BTO})/a_\parallel = -0.139\%$, where a_0^{Fe} (0.4053 nm along Fe[110]) and a_0^{BTO} (0.3992 nm along BTO[100]) are free lattice constant of Fe and BTO, respectively. $a_\parallel \approx \frac{a_0^{Fe}d_{Fe} + a_0^{BTO}d_{BTO}}{d_{Fe} + d_{BTO}} = 0.3998$ nm is the in-plane lattice constant of epi-bilayer.

$$\Delta P_{iz} = \sum_{\xi} c_{3\xi} u_{i\xi}^{\mathrm{FE}} + \epsilon_0 \chi^{\mathrm{e}} E_i, \tag{1}$$

where $c_{3\xi}$ ($\xi = 1, 2, 3$) is the improper piezoelectric tensors [52], ϵ_0 is the free space permittivity, and χ^{e} is the electric susceptibility. The effective electric field E_i derives as $E_i = \delta F_{\mathrm{FE}}/\delta \mathbf{P}_i$, where F_{FE} is being the coarse-grained FE free energy [18], $F_{\mathrm{FE}} = F_{\mathrm{EE}} + F_{\mathrm{DDI}}$. The elastic Gibbs function F_{EE} corresponding to the tetragonal phase of BaTiO$_3$ reads [18, 41]

$$F_{\mathrm{EE}} = -\frac{\alpha}{2} \sum_i \mathbf{P}_i^2 + \frac{\beta}{4} \sum_i \mathbf{P}_i^4 + \kappa \sum_i (\mathbf{P}_i - \mathbf{P}_{i-1})^2$$
$$+ \frac{1}{\epsilon_0} \sum_i [c_{31}(u_{ix}^{\mathrm{FE}} + u_{iy}^{\mathrm{FE}}) + c_{33} u_{iz}^{\mathrm{FE}}] P_{iz} + \sum_i \frac{1}{2} C_{11}^{FE} \mathbf{u}_i^{\mathrm{FE}} \cdot \mathbf{u}_i^{\mathrm{FE}}. \tag{2}$$

Here we accounted for the symmetry $c_{31} = c_{32}$. The stiffness coefficient of the FE part is C_{11}^{FE}. F_{DDI} is the long range FE dipole–dipole interaction which has the usual form

$$F_{\mathrm{DDI}} = \frac{1}{4\pi \epsilon_{\mathrm{FE}} \epsilon_0} \sum_{i \neq k} \left[\frac{\mathbf{P}_i \cdot \mathbf{P}_k - 3(\mathbf{P}_i \cdot \mathbf{e}_{ik})(\mathbf{e}_{ik} \cdot \mathbf{P}_k)}{r_{ik}^3} \right], \tag{3}$$

where ϵ_{FE} is the FE permittivity, r_{ik} is the distance between $\mathbf{P}_i$ and $\mathbf{P}_k$, and $\mathbf{e}_{ik}$ is the unit vector joining the two dipoles.

Analogously, for the FM energy density the relation applies $F_{\mathrm{FM}} = F_{\mathrm{XC}} + F_{\mathrm{MMI}}$. F_{XC} consists of the nearest-neighbor exchange interaction (A-term) between $\mathbf{M}_j$ and $\mathbf{M}_{j+1}$, the uniaxial magneto-crystalline anisotropy contributions (K_1-term), and the (magneto-) elastic energies,

$$F_{\mathrm{XC}} = -\frac{A}{a^2 M_S^2} \sum_j \mathbf{M}_j \cdot \mathbf{M}_{j+1} - \frac{K_1}{M_S^2} \sum_j \mathbf{M}_{jz}^2$$
$$+ B_1 \sum_{j,\xi} u_{j\xi}^{\mathrm{FM}} \left(\frac{M_{i\xi}^2}{M_S^2} - \frac{1}{3} \right) + \frac{1}{2} \sum_j C_{11}^{\mathrm{FM}} \mathbf{u}_j^{\mathrm{FM}} \cdot \mathbf{u}_j^{\mathrm{FM}}. \tag{4}$$

M_s is the saturation magnetization. The anisotropy K_1 depends on the FM film thickness d_{FM}, $K_1 = (K_s/d_{\mathrm{FM}} - \mu_0 M_s^2/2)$, where K_s describes the surface anisotropy contributions that are significant for ultra-thin film tending to align the magnetization normal to the surface, whereas, $\mu_0 M_s^2/2$ denotes the demagnetization field that is equivalent to an easy in-plane contribution. B_1 and C_{11}^{FM} respectively denote the magneto elastic constants and elastic moduli of the FM layer. The magnetic dipole–dipole interaction F_{MMI} is

$$F_{\mathrm{MMI}} = \frac{\mu_0}{4\pi} \sum_{j \neq l} \left[\frac{\mathbf{M}_j \cdot \mathbf{M}_l - 3(\mathbf{M}_j \cdot \mathbf{e}_{jl})(\mathbf{e}_{jl} \cdot \mathbf{M}_l)}{r_{jl}^3} \right], \tag{5}$$
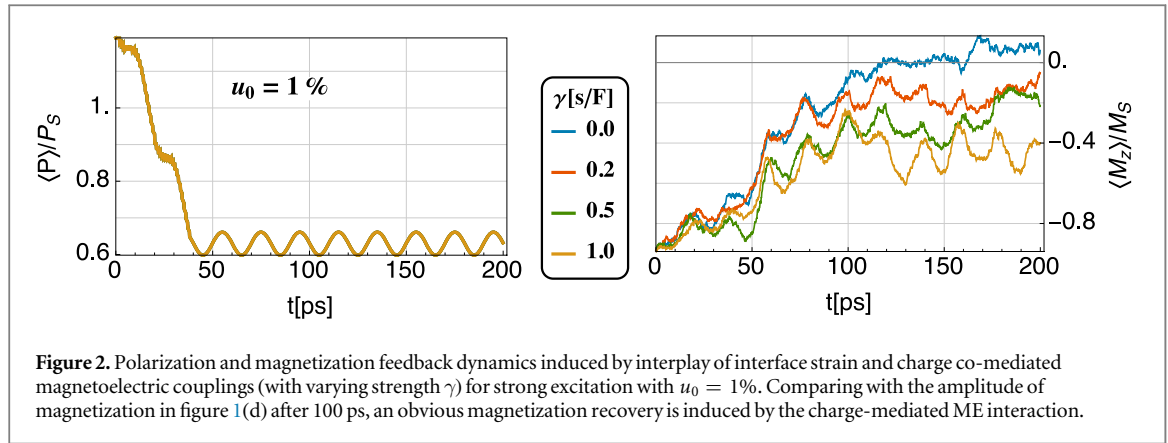
where μ_0 is the magnetic permeability constant.

We are targeting exclusively ps-ns time scales, i.e. the range for laser-induced fs-demagnetization [34] is not discussed here. The dynamics of orbital degrees of freedom is therefore not explicitly taken into account (i.e., they are assumed to have relaxed to the dynamics considered here). The material parameters for the FE subsystem are chosen as $\alpha = 2.77 \times 10^7$ Vm C^{-1} [53], $\beta = 1.70 \times 10^8$ Vm^5 C^{-3} [53], $\kappa = 1.0 \times 10^8$ Vm C^{-1} [26], $P_d = 0.499$C m^{-2} [18], and $C_{11}^{\mathrm{FE}} = 1.78 \times 10^{11}$ N m^{-2} [54]. The improper piezoelectric constants are set as those of BTO [52]: $c_{31} = 0.3$ C m^{-2}, $c_{33} = 6.7$ C m^{-2}, and the Poisson ratio $n = 0.64$ [49]. Further material parameters concerning the FM layer are iron, i.e., $\lambda = 2.07 \times 10^{-5}$ along Fe [100], $B_1 = -2.95 \times 10^6$ N m^{-2}, $C_{11}^{\mathrm{FM}} = 2.41 \times 10^{11}$ N m^{-2} [55], $A = 2.1 \times 10^{-11}$ J m^{-1} [56], $K_1 = 4.8 \times 10^4$ J m^{-3} [56], $M_s = 1.71 \times 10^6$ A m^{-1} [56]. We assume that none of these parameters changes during the dynamics of interest here.

From the symmetry point of view, the space-inversion symmetry and the time-reversal symmetry are intrinsically broken at the FE/FM interface [57, 58], the MF coupling is thus restricted to the region in the vicinity of the interface,

$$F_{\mathrm{ME}} = \gamma \mathbf{P}_1 \cdot \mathbf{M}_1 - \frac{3}{2} \lambda \sigma \cos^2 \phi. \tag{6}$$

The first γ-term has its origin in a magnon-driven, direct ME interaction in the vicinity of the FE/FM interface acting within the spin-diffusion length on the order of nanometers [27, 45]. γ is the coupling strength in unit of s F^{-1}. Given that the spin-diffusion length is around 8.5 nm in Fe [59], the linear direct ME coupling is assumed to only involve the interfacial nearest neighbor cells, i.e. the FE polarization $\mathbf{P}_1$ and FM magnetization $\mathbf{M}_1$, only. The second λ-term involves piezoelectricity and the magnetostriction at the interface, associated with an additional uniaxial anisotropy energy for the FM layer [14, 18, 55]. λ is the average magnetostriction coefficient, and ϕ is the angle between the magnetization $\mathbf{M}$ and the direction of the stress $\boldsymbol{\sigma}$ across the interface, $\boldsymbol{\sigma} = -C_{11}^{\mathrm{FE}} \mathbf{u}_1^{\mathrm{FE}} + C_{11}^{\mathrm{FM}} \mathbf{u}_1^{\mathrm{FM}}$. The in-plane *static* stress at the interface is assumed to be balanced due to the lattice

Figure 2. Polarization and magnetization feedback dynamics induced by interplay of interface strain and charge co-mediated magnetoelectric couplings (with varying strength γ) for strong excitation with $u_0 = 1\%$. Comparing with the amplitude of magnetization in figure 1(d) after 100 ps, an obvious magnetization recovery is induced by the charge-mediated ME interaction.

deformation. Taking that $\lambda > 0$ in our case, a negative film stress ($\sigma < 0$) on FM layer favors $\phi = \pi/2$ which means an in-plane magnetization while $\sigma > 0$ favors an out-of-plane magnetization with $\phi = 0$. It should be noted that we focus on thin FM films, the indirect high-order ME coupling, such as a spin-motive force resulting from the non-equilibrium magnetic domain wall dynamics [60], is disregarded here. Other cases of strains can be treated similarly.

As demonstrated by trXRD experiments [36–38, 61], except for a static strain due to the lattice mismatch, electronic excitation by an ultrafast pump pulse generates *dynamic* transient strain propagating through the FE/FM films, directly affecting the dynamics of the magnetization and polarization. Here we assume that an applied optical pulse is exclusively absorbed in Fe layer, changing so the electronic configuration of the absorbing material and generating a transient stress that results in a displacive excitation of phonons in the Fe/BTO systems through the electron–phonon coupling. The expansion front with an amplitude $u_f(0, 0)$ starts at time $t = 0$ from the top air-Fe interface, enters into the Fe and BTO layers with the respective sound velocity ($v_{Fe} = 5130$ m s^{-1} and $v_{BTO} = 5437$ m s^{-1}, respectively) and arrives at the surface of the substrate after $\Delta t = d_{FM}/v_{Fe} + d_{FE}/v_{BTO} \approx 20$ ps. At the BTO/substrate interface, the strain front is reflected from the substrate surface and backs into the Fe/BTO heterostructure, encountering the incoming strain wave, and then launching a coherent acoustic standing wave with the wave vector $k = 1/(d_{FM} + d_{FE})$. Such a coherence lattice motion is manifested in fast oscillation (with system-size-determined period $T = \Delta t$) of FE polarization and FM magnetization due to piezoelectricity and magnetostriction respectively, as shown in figures 1 and 2. Furthermore, the polarization/magnetization dynamics are coupled to each other at the interface due to the ME coupling, which gives rise to marked changes in FE/FM response since the surface contribution to the free energy plays an important role for nanostructures.

The time evolution of the strain wave depends significantly on the pump fluences [37]. Without loss of generality two limiting cases are to be considered:

(i) *Strong excitation.* For large pump fluences, the heterostructures may suddenly deform within femtoseconds. For ps dynamics, the strain front amplitude acts promptly as
$u_f(z, t) = -u_0 \sin(2\pi kz - 2\pi\omega t + \pi/2)$ (i.e., $-u_0$ for $t = 0$) with the frequency $\omega = 1/T$. The strain standing wave reads $u_s(z, t) = -2u_0[1 - \cos(2\pi kz)\sin(2\pi\omega t)]$ after $t = 2T = 40$ ps.

(ii) *Weak excitation.* For moderate pump fluences the expansion front $u_f(z, t) = u_0 \sin(2\pi kz - 2\pi\omega t)$ travels within FE/FM heterostructures leading to the standing wave $u_s(z, t) = 2u_0 \sin(2\pi kz)\cos(2\pi\omega t)$. The general pump case is a super-position of these two cases.

Numerical results and analysis

The MF dynamics is studied by kinetic Monte Carlo simulations [18, 62] with open boundary condition at room temperature (300 K) for tetragonal BTO phase. The kinetic Monte Carlo method is advantageous in that it is computationally more tractable than a direct solution of the coupled Landau–Lifshitz–Gilbert/Landau–Khalatnikov equations that we examined earlier [26]. The magnetic moments $\mathbf{M}_j$ are understood as three-dimensional unit vectors, which are updated coherently, i.e., at each trial step the direction of new $\mathbf{M}_j$ is limited within a cone around the initial spin direction [63]. The maximum angle θ_{max} of the cone is determined by means of a feedback algorithm so that the number of accepted spin modifications is just half the total number of equilibrium configurations at a given temperature before the x-ray diffraction [64]. In experiments with BTO, the FE dipoles in the tetragonal phase are along the [001] direction and are thus assumed to be bi-directional vectors. The remanent polarization is $\mathbf{P}_s$ and the field-induced deviation is ΔP_t and is given by equation (1)
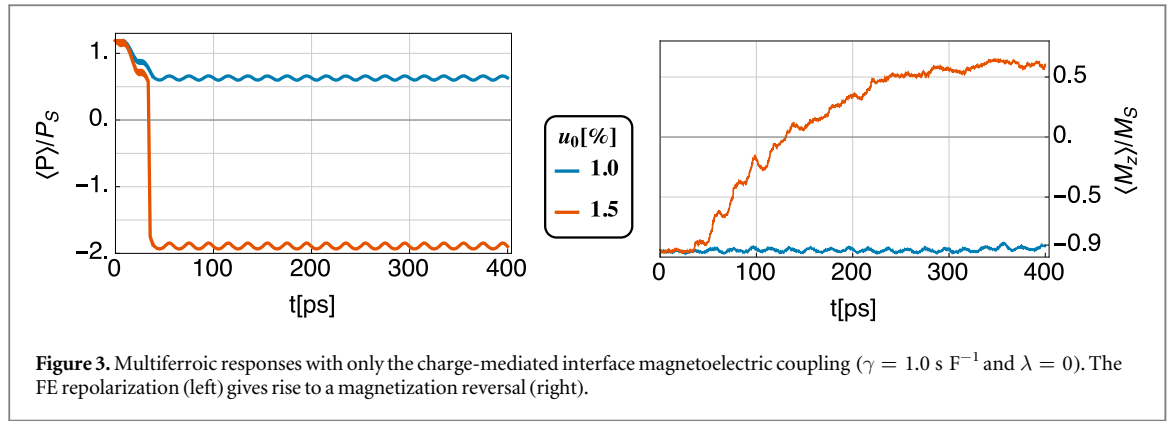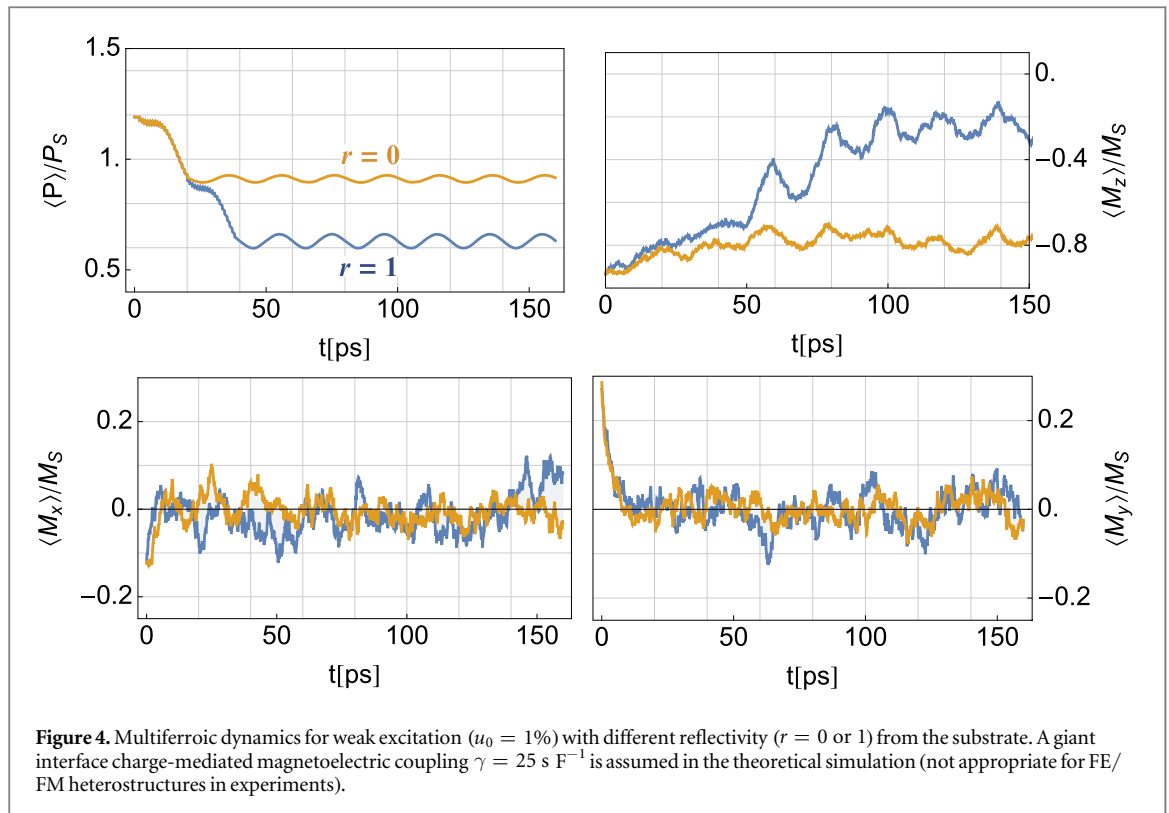
Figure 3. Multiferroic responses with only the charge-mediated interface magnetoelectric coupling ($\gamma = 1.0$ s F^{-1} and $\lambda = 0$). The FE repolarization (left) gives rise to a magnetization reversal (right).

[65, 66]. During the simulations, the MF equilibrium at 300 K is at first established with $\Delta P_i = 0$, θ_{max} is determined. Then a transmit strain along the chain is turned on at $t = 0$ and it propagates through the multiferrroic chain. The strain wave and all induced FE dipole moments are updated with the time step $\tau_0 = 0.1 ps$, which is also taken as the *time unit* of Monte-Carlo algorithm [62]. To reduce possible random errors, the data are collected and averaged for 4000 independent runs.

As discussed after equation (6), the MF dynamics is in general strain and charge mediated. However, for the type of excitations considered here strain is a key factor. For an insight into various mechanisms, at first only strain-mediated ME interaction is considered. Figure 1 shows transient changes in the averaged polarization and magnetization for a strong pump pulse with 100% reflectivity from the substrate. FE polarizations are strongly suppressed by the photo-induced stress (figure 1 (c)), with/without the strain-mediated ME couplings. There are two distinguishable change steps (at $t = 20$ ps and $t = 40$ ps, respectively) corresponding to π-phase shifts between the incoming expansion wave and the reflected front before forming a standing strain wave. As the peak strain exceeds 1.4% a critical point is arrived. The negative piezoelectric contribution ΔP_i exceeds the permanent dipole $\mathbf{P}_s$, a full FE polarization reversal is then induced by the strong piezoelectricity within 40 ps. Experimentally such a strain-induced ultrafast characterization of polarization dynamics has indeed been observed in a PbZr$_{0.2}$Ti$_{0.8}$O$_3$/SrRuO$_3$ superlattice [37, 38, 61], where the FE dynamics was traced back to the anharmonic coupling of the tetragonal distortion and the FE soft phonon mode in PZT. For the FM subsystem in general, an optical excitation generates a time-dependent magneto-elastic anisotropy making the normal z-axis magnetically harder with the increase of the amplitude of strain wave u_0 (see equation (4)). This leads to a fast-oscillation but a relatively weak and slow reduction of the normal magnetization $\langle M_z \rangle$ (see figure 1 (d)). Upon accounting for the uniaxial interfacial magnetic anisotropy (λ-term in equation (6)) that stems from the stress σ across the FE/FM interface, we find a magnetic transition from FM to paramagnetic state (i.e., $\langle M_z \rangle \to 0$) in 100 ps range (figure 1 (d)). We recall that we adopt a phenomenology based on coarse-grained order parameters that formally result from an averaging over microscopic quantities over an $5 \times 5 \times 5$ nm^3 cell. As mentioned above the time scale and the origin of the demagnetization processes in our system are quite different from the conventional fs to ps laser-induced demagnetization dynamics [34, 67]. Furthermore, the lattice deformation $u_i < 0$ results in a surface tensile rather than compressive strain to Fe along the z-axis. So, such a collapse of magnetic order does not correspond to the case of '*Iron under pressure*' [68–70], where magnetic transition is simultaneously accompanied by a high *pressure* bcc to hcp structure transition. Here the magnetic collapse phenomenon is attributable to the *extraordinarily* hardening of the magnetic uniaxial $\boldsymbol{\sigma}$-axis. As strain wave propagates through the heterostructures, the interface stress $\boldsymbol{\sigma}$ acting on Fe is rapidly oscillating and reaches a giant value, for instance $\sigma = -16.5$ GPa with $u_0 = 1\%(2\%)$ at $t = 55(15)$ ps, which makes the stress axis extremely hard, altering substantially the FM order along the magnetocrystalline axis within tens of picoseconds. The in-plane magnetization is then favorable. Considering the SO(2) rotational symmetry of the magnetoelastic anisotropy (B_1-term in equation (4)) about the $\mathbf{e}_z$-axis, however, there is no preferred easy axis in the normal plane to the direction of surface stress, resulting in a rotational in-plane anisotropy. The numerical calculations confirm that the in-plane averaged magnetization $\langle M_x \rangle$ and $\langle M_y \rangle$ present a noise-like dynamic behavior, we thus have an ultrafast interface strain-driven demagnetization in a MF FE/FM heterostructure.

For a more complete scenario of ultrafast MF dynamics, another interfacial ME coupling induced by the spin-polarized screening charges should be considered [27]. Different from strain-mediated MF interaction, the charge-mediated, magnon-driven ME effect couples directly the dynamics of FE polarization and FM magnetization and favors antiparallel alignment perpendicular to the interface. Taking into account that the strength of direct ME interaction is around 1 s F^{-1} in metallic FM film [27, 43, 45], such electrically controllable effective magnetic field generated by the non-vanishing normal FE polarization gives rise to an induced magnetization along $\langle P_z \rangle$ from the paramagnetic state, as evidenced in figure 2. On the other hand, with strain

Figure 4. Multiferroic dynamics for weak excitation ($u_0 = 1\%$) with different reflectivity ($r = 0$ or 1) from the substrate. A giant interface charge-mediated magnetoelectric coupling $\gamma = 25$ s F^{-1} is assumed in the theoretical simulation (not appropriate for FE/FM heterostructures in experiments).

amplitude $u_0 = 1\%$, the coupling strength $\gamma = 1$ s F^{-1} is insufficient to produce considerable feedback changes in FE polarization. The FE/FM feedback is only pronounced, for a large coupling γ. The pre-contact FE cell diminishes in magnitude and then flips its direction for $\gamma > 14$ s F^{-1}, causing the emergence of the re-polarized FE. Simultaneously, due to the interplay of the interface strain and charge-mediated magnetic anisotropy, the FM part recovers remnant magnetism, which favors the opposite orientation of the polarization as expected.

Given the large mismatch in stiffness coefficients between FE/FM films [25] or appropriately fabricated FM/FE crystal orientation [44], the magnetostrictive effects can be minimized, the direct electric-field effects would then dominate the MF dynamics. In figure 3 the MF responses, driven by charge-mediated ME interaction *only*, are demonstrated. As one can see, the propagating mechanical stress with the strain-front 1.5% reverse the FE polarization and consequently the FM magnetization due to the requirement of the antiparallel configuration between the polarization and magnetization by the direct charge-mediated ME coupling.

To explore the FE/FM feedback response in the case of *weak excitation*, a very large interface charge-mediated ME coupling $\gamma = 25$ s F^{-1} is assumed in the theoretical simulation. The system exhibits demagnetization due to the dynamic strain effect as well (see figure 4), but FE re-polarization vanishes even with such an unrealistic (giant) interface charge-mediated ME coupling, though the FE/FM feedback are still present and induces a quasi-square-pulse FE dynamic behavior.

Conclusions

We proposed and theoretically realized a scheme for studying ultrafast dynamics in a composite MF heterostructure related to Fe/BaTiO$_3$. Based on the piezoelectricity and the magnetostriction resulting from a coherent lattice motion in the FE and the FM launched by a pump laser pulse, the critical amplitude of the strain front 1.4% gives rise to a complete switching of the bipolar FE polarization, while at the same time for zero ME coupling of any type it has low impact on the FM order (figures 1(c) and (d)). Only in the presence of the strain-mediated ME coupling (second term of equation (6)) the total out-of-plane magnetization becomes supressed (figure 1(d)). The effect of the charge-mediated coupling (first term of equation (6)) is opposite. It results in a partial recovery of the total M_z-component on the time scale of about 200 ps (figure 2). It should be noted that the reflectivity of propagating strain wave from the substrate is not necessary for the ultrafast MF dynamics but it indeed enhances the studied effects (see figure 4). In addition, it is numerically evident that such ultrafast ME dynamics are general in FE/FM heterostructures containing strong piezoelectric FE subsystem, such as BaTiO$_3$ and PbTiO$_3$ [52]. The results indicate the potential of MF composite for photo-operated high-speed devices.

Acknowledgments

References

[1] Eerenstein W, Mathur N D and Scott J F 2006 *Nature* **442** 759
[2] Ramesh R and Spaldin N A 2007 *Nat. Mater.* **6** 21–9
[3] Gajek M, Bibes M, Fusil S, Bouzehouane K, Fontcuberta J, Barthélémy A and Fert A 2007 *Nat. Mater.* **6** 296
[4] Vaz C A F, Hoffman J, Ahn C H and Ramesh R 2010 *Adv. Mater.* **22** 2900
[5] Spaldin N A, Cheong S W and Ramesh R 2010 *Phys. Today* **10** 38
[6] Velev J P, Jaswal S S and Tsymbal E Y 2011 *Phil. Trans. R. Soc.* A **369** 3069
[7] Lu X L, Kim Y, Goetze S, Li X G, Dong S, Werner P, Alexe M and Hesse D 2011 *Nano Lett.* **11** 3202
[8] Pantel D, Goetze S, Hesse D and Alexe M 2012 *Nat. Mater.* **11** 289
[9] Vaz C A F 2012 *J. Phys.: Condens. Matter* **24** 333201
[10] Fusil S, Garcia V, Barthélémy A and Bibes M 2014 *Ann. Rev. Mater. Res.* **44** 91
[11] Liu M and Sun N X 2014 *Phil. Trans. R. Soc.* A **372** 20120439
[12] Tokura Y, Seki S and Nagaosa N 2014 *Rep. Prog. Phys.* **77** 076501
[13] Bibes M and Barthélémy A 2008 *Nat. Mater.* **7** 425
[14] Sahoo S, Polisetty S, Duan C-G, Jaswal S S, Tsymbal E Y and Binek C 2007 *Phys. Rev.* B **76** 092108
[15] Taniyama T, Akasaka K, Fu D-S and Itoh M 2009 *J. Appl. Phys.* **105** 07D901
[16] Venkataiah G, Shirahata Y, Itoh M and Taniyama T 2011 *Appl. Phys. Lett.* **99** 102506
[17] Valencia S *et al* 2011 *Nat. Mater.* **10** 753
[18] Jia C-L, Sukhov A, Horley P P and Berakdar J 2012 *Europhys. Lett.* **99** 17004
[19] Duan C-G, Jaswal S S and Tsymbal E Y 2006 *Phys. Rev. Lett.* **97** 047201
[20] Fechner M, Ostanin S and Mertig I 2010 *J. Phys.: Conf. Ser.* **200** 072027
[21] Wang Y, Zhang N, Berakdar J and Jia C L 2013 *Appl. Phys. Lett.* **103** 052903
[22] Chotorlishvili L, Khomeriki R, Sukhov A, Ruffo S and Berakdar J 2013 *Phys. Rev. Lett.* **111** 117202
[23] Lee J, Na Sai T Y, Cai Q, Niu and Demkov A A 2010 *Phys. Rev.* B **81** 144425
[24] Meyerheim H L, Klimenta F, Ernst A, Mohseni K, Ostanin S, Fechner M, Parihar S, Maznichenko I V, Mertig I and Kirschner J 2011 *Phys. Rev. Lett.* **106** 087203
[25] Mardana A, Ducharme S and Adenwalla S 2011 *Nano Lett.* **11** 3862
[26] Sukhov A, Jia C-L, Horley P P and Berakdar J 2010 *J. Phys.: Condens. Matter* **22** 352201
[27] Jia C L, Wei T L, Jiang C J, Xue D S, Sukhov A and Berakdar J 2014 *Phys. Rev.* B **90** 054423
[28] Borisov P, Hochstrat A, Chen X, Kleemann W and Binek C 2005 *Phys. Rev. Lett.* **94** 117203
[29] Laukhin V *et al* 2006 *Phys. Rev. Lett.* **97** 227201
[30] Wu S M, Cybart S A, Yu P, Rossell M D, Zhang J X, Ramesh R and Dynes R C 2010 *Nat. Mater.* **9** 756
[31] Wen H, Chen P, Cosgriff M P, Walko D A, Lee J H, Adamo C, Schaller R D, Ihlefeld J F, Dufresne E M, Schlom D G *et al* 2013 *Phys. Rev. Lett.* **110** 037601
[32] Schick D, Herzog M, Wen H, Chen P, Adamo C, Gaal P, Schlom D G, Evans P G, Li Y and Bargheer M 2014 *Phys. Rev. Lett.* **112** 097602
[33] Sheu Y M, Trugman S A, Yan L, Chuu C-P, Bi Z, Jia Q X, Taylor A J and Prasankumar R P 2013 *Phys. Rev.* B **88** 020101
[34] Kirilyuk A, Kimel A and Rasing T 2010 *Rev. Mod. Phys.* **82** 2731 references therein
[35] Elsaesser T 2009 *Appl. Phys.* A **96** 1 and references therein
[36] Bargheer M, Zhavoronkov N, Gritsai Y, Woo J C, Kim D S, Woerner M and Elsaesser T 2004 *Science* **306** 1771
[37] Korff-Schmising C v, Bargheer M, Kiel M, Zhavoronkov N, Woerner M, Elsaesser T, Vrejoiu I, Hesse D and Alexe M 2006 *Phys. Rev.* B **73** 212202
[38] Korff Schmising C v, Bargheer M, Kiel M, Zhavoronkov N, Woerner M, Elsaesser T, Vrejoiu I, Hesse D and Alexe M 2007 *Phys. Rev. Lett.* **98** 257601
[39] Woerner M, Korff Schmising C, Bargheer M, Zhavoronkov N, Vrejoiu I, Hesse D, Alexe M and Elsaesser T 2009 *Appl. Phys.* A **96** 83
[40] Nan T *et al* 2014 *Sci. Rep.* **4** 3688
[41] Sukhov A, Horley P P, Jia C L and Berakdar J 2013 *J. Appl. Phys.* **113** 013908
     Sukhov A, Jia C L, Chotorlishvili L, Horley P P, Sander D and Berakdar J 2014 *Phys. Rev.* B **90** 224428
[42] Mardana A, Ducharme S and Adenwalla S 2011 *Nano Lett.* **11** 3862
[43] Jedrecy N, von Bardeleben H J, Badjeck V, Demaille D, Stanescu D, Magnan H and Barbier A 2013 *Phys. Rev.* B **88** 121409
[44] Zhang C, Wang F, Dong C, Gao C, Jia C, Jiang C and Xue D 2015 *Nanoscale* **7** 4187
[45] Jia C, Wang F, Jiang C, Berakdar J and Xue D 2015 *Sci. Rep.* **5** 11111
[46] Kovalenko O, Pezeril Th and Temnov V V 2013 *Phys. Rev. Lett.* **110** 266602
[47] Jia C-L, Sukhov A, Horley P P and Berakdar J 2011 *J. Phys. Conf. Ser.* **303** 012061
[48] Ibach H 2006 *Physics of Surfaces and Interfaces* (Berlin: Springer)
[49] Neaton J B, Hsueh C-L and Rabe K M 2012 *MRS Proc.* **718** 311
[50] Horley P P, Sukhov A, Jia C, Martnez E and Berakdar J 2012 *Phys. Rev.* B **85** 054401
[51] Martin R M 1972 *Phys. Rev.* B **5** 1607
[52] Ederer G and Spaldin N 2005 *Phys. Rev. Lett.* **95** 257601
[53] Hlinka J and Márton P 2006 *Phys. Rev.* B **74** 104104
[54] Rabe K, Ahn Ch H and Triscone J-M (ed) 2007 *Physics of Ferroelectrics: A Modern Perpective* (Berlin: Springer)
[55] Chikazumi S 2002 *Physics of Ferromagnetism* (New York: Oxford University Press)
[56] Coey J M D 2010 *Magnetism and Magnetic Materials* (Cambridge: Cambridge University Press)

[57] Eerenstein W, Mathur N D and Scott J F 2006 *Nature* **442** 759

[58] Rondinelli J M, Stengel M and Spaldin N A 2008 *Nat. Nanotechnology* **3** 46

[59] Bass J and Pratt W P Jr 2007 *J. Phys.: Condens. Matter* **19** 183201

[60] Barnes S and Maekawa S 2007 *Phys. Rev. Lett.* **98** 246601

[61] Woerner M, Korff Schmising C v, Bargheer M, Zhavoronkov N, Vrejoiu I, Hesse D, Alexe M and Elsaesser T 2009 *Appl. Lett.* A **96** 83

[62] Landau D P and Binder K 2009 *A Guide to Monte-Carlo Simulations in Statistical Physics* (Cambridge: Cambridge University Press)

[63] Hinzke D and Nowak U 1998 *Phys. Rev.* B **58** 265

[64] Serena P A, García N and Levanyuk A 1993 *Phys. Rev.* B **47** 5027

[65] Potter B G Jr, Tuttle B A and Tikare V 2000 *AIP Conf. Proc.* **535** 173

[66] Gao X S, Liu J-M, Chen X Y and Liu Z G 2000 *J. Appl. Phys.* **88** 4250

[67] Kazantseva N, Nowak U, Chantrell R W, Hohlfeld J and Rebei A 2008 *Europhys. Lett.* **81** 27004

[68] Shimizu K, Kimura T, Furomoto S, Takeda K, Kontani K, Onuki Y and Amaya K 2001 *Nature* **412** 316

[69] Steinle-Neumann G, Cohen R E and Stixrude L 2004 *J. Phys.: Condens. Matter* **16** S1109

[70] Monza A, Meffre A, Baudelet F, Rueff J-P, d'Astuto M, Munsch P, Huotari S, Lachaize S, Chaudret B and Shukla A 2011 *Phys. Rev. Lett.* **106** 247201